ICES Journal of Marine Science, 60: 429–434. 2003
doi:10.1016/S1054–3139(03)00002-X

Reconciling theoretical versus empirical target strengths of krill: effects of phase variability on the distorted-wave Born approximation

David A. Demer and Stéphane G. Conti

Demer, D. A., and Conti, S. G. 2003. Reconciling theoretical versus empirical target strengths of krill: effects of phase variability on the distorted-wave Born approximation. – ICES Journal of Marine Science, 60: 429–434.

A model was recently proposed to predict the target strengths (TS) of Antarctic krill, *Euphausia superba*, versus incidence angle (θ) (Deep Sea Res. II 45(7) (1998) 1273). Based on the distorted-wave Born approximation (DWBA), the model depends on the coherent summation of scattering from elements of a discretized-bent cylinder. It was empirically validated at 120 kHz near-broadside incidence ($\theta \approx 90^\circ$), but large discrepancies were observed at other angles away from the main lobe. As the side-lobe measurements were both higher than the model predictions and above the noise floor, the authors noted that the differences were not entirely due to noise. In this study, the accuracy of the DWBA model is further explored. Results indicate that phase variability in the scatter from elements of a discretized-bent cylinder (krill model) causes a dramatic flattening in the side-lobe regions of TS(θ), while negligibly affecting the main scattering lobe. These results are consistent with the krill TS measurements reported by McGehee *et al.* Thus, by accounting for phase variability in the solution of the DWBA model, a more accurate and thus practical tool is developed for predicting krill TS.

Keywords: phase variability, krill, target strength.

Received 25 October 2002; accepted 19 December 2002.

D. A. Demer: Southwest Fisheries Science Center, 8604 La Jolla Shores Drive, La Jolla, CA 92037, USA. Correspondence to D. A. Demer: tel.: +858 546 5603; fax: +858 546 5608; e-mail: david.demer@noaa.gov.

Introduction

Because Antarctic krill, *Euphausia superba*, form the basis for the food web in the Southern Ocean and are the target of a large fishery, there has been much international endeavor to map their distribution and quantify their abundance (Hewitt *et al.*, 2002). Accurate knowledge of the acoustic target strengths (TS) of individual krill is a vital component of the analyses of these surveys employing echo-integration methods. Greene *et al.* (1991) proposed a linear model of TS versus the logarithm of standard length (L), which is based on measurements (Wiebe *et al.*, 1990) of a variety of crustacean zooplankton but not Antarctic krill. However, using TS measurements of live krill, the model was corroborated at an acoustical frequency (f) of 120 kHz for a small number of L (Foote *et al.*, 1990; Hewitt and Demer, 1991). Deemed the best available model at the time, the Antarctic Treaty Organization's Committee for the Conservation of Antarctic Marine Living Resources adopted the Greene *et al.* model as an international standard for estimating krill biomass (SC-CAMLR, 1991).

Motivated by observations that were inconsistent with the Greene *et al.* model's predictions, Demer and Martin (1995) highlighted the changes in TS due to variations in animal shape, morphology, and orientation, for which the model does not take account. Moreover, Demer (in press) provided evidence that the Greene *et al.* model has significantly reduced accuracy in the Rayleigh and Mie scattering regimes. In light of these concerns, McGehee *et al.* (1998) used the distorted-wave Born approximation (DWBA; Morse and Ingard, 1968) to model the TS of Antarctic krill versus f, and animal density (ρ), sound speed (c), L, shape (S), and angle of orientation relative to the incident wave (θ). Using krill TS measurements at $f = 120$ kHz, they also validated the DWBA model on the main scattering lobe, near-broadside incidence. Unfortunately, at other angles (i.e. in the side-lobes), large discrepancies (5–20 dB) were observed between measurement and theory. The effects of noise could not entirely explain the nonconforming measurements because they were both higher than the model predictions and above the noise floor (McGehee *et al.*, 1998). The significance of these differences was not assigned but the authors highlighted the need for accurate information about krill orientations.

Unfortunately, there is a paucity of information about the naturally occurring orientations of Antarctic krill. Possibly, the best quantitative information comes from Kils (1981), who meticulously quantified the orientation distributions of krill swimming in an aquarium. However, solving the DWBA model with the orientation distributions from Kils ($\theta = N(45.3°, 30.4°)$), McGehee *et al.* (1998) showed expected values of krill TS to be 6–8 dB lower than that predicted by the Greene *et al.* model and the *in situ* TS measurements of krill by Hewitt and Demer (1991). This difference is highly significant because use of the DWBA model solved with Kils' krill orientation distribution would result in an increase of roughly a factor of 5 in biomass estimates relative to the ones computed with the Greene *et al.* model. For TS predictions to approach the *in situ* measurements, the DWBA must be solved with an improbably narrow distribution of krill orientations centered on normal incidence.

To explain this important inconsistency it should be noted first that the DWBA model was not successfully validated for angles greater than about 15–30° off normal incidence ($\theta \approx 90°$) and the computations in McGehee *et al.* (1998) did not account for the stochastic nature of sound scattering. They made numerous measurements at other angles but the TS(θ) was virtually constant in the side-lobes, at a level 5–10 dB above the measured noise floor (Figure 1). This analysis aims to reconcile the TS predictions by the DWBA model and the measurements of krill TS versus θ in McGehee *et al.* (1998). Success in this endeavor may improve the accuracy of the DWBA model and thus provide a more dependable tool for estimating TS of Antarctic krill for naturally occurring distributions of angles of incidence, animal shapes, sizes, and material properties, and over a range of acoustical frequencies.

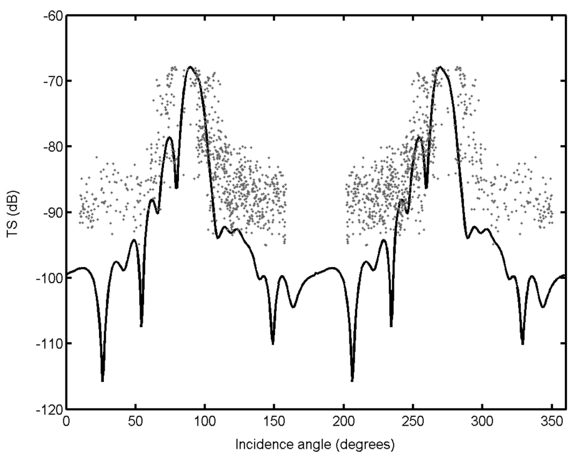

Figure 1. The DWBA model (solid line), and the experimental TS of Animal 1 (dots) from McGehee *et al.* (1998). In the side-lobes, when the backscattered signal from the krill is about 10–15 dB above the noise floor (−95 dB), the agreement between the measurements and the DWBA theory ends.

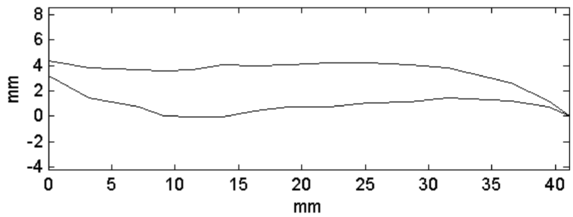

Figure 2. The generic shape for *E. superba* from McGehee *et al.* (1998). Model parameters are listed in Table 3 of their article.

Methods

As in McGehee *et al.* (1998), the DWBA (Morse and Ingard, 1968), is used to model acoustical scattering from krill which have mass density (ρ) and sound speed (c) values close to those of the surrounding seawater medium. The backscattering form function for part j of the scatterer field is

$$f_{bs_j}(\theta) = \frac{k_1^2}{4\pi} \iiint_{V_j} [\gamma_\kappa - \gamma_\rho] \exp(-i2\vec{k}_i \vec{r}_0)\, dV, \tag{1}$$

where $k_1 = 2\pi f/c$ is the acoustical wave number,

$$\vec{k}_i = k_1 \begin{bmatrix} \sin\theta \\ 0 \\ \cos\theta \end{bmatrix},$$

$\vec{r}_0$ is the position vector, $\gamma_\kappa = (\rho_1 c_1^2/\rho_2 c_2^2) - 1$, and $\gamma_\rho = (\rho_2 - \rho_1)/\rho_2$. The subscript 1 denotes the ambient seawater and 2 the krill.

Stanton *et al.* (1998) stated that Equation (1) can be solved as a line-integral if the krill shape is approximated by a discretized-bent cylinder, elements noted j, having radii (a_j) and positions ($\vec{r}_{pos}$) along a central line

$$f_{bs_j}(\theta) = \frac{k_1}{4} \int [\gamma_\kappa - \gamma_\rho] \exp(-2i\vec{k}_i \vec{r}_0) \times \frac{a_j J_1(2k_2 a_j \cos\beta_{tilt})}{\cos\beta_{tilt}} dr_0, \tag{2}$$

where J_1 is the Bessel function of the first kind of order 1, and β_{tilt} is the angle between the cylinder and the incident wave. Using N = 15 cylinders with relative a_j and $\vec{r}_{pos_j}$ (Figure 2; generic krill shape and number of cylinders from McGehee *et al.*, 1998), the form function is obtained by summing the components from each of the scattering elements

$$f_{bs}(\theta) = \sum_{j=1}^{N} f_{bs_j}(\theta). \tag{3}$$

At broadside incidence, the relatively high backscattered level (see Figure 1) is mostly due to constructive interference. At other angles, the interference can be mostly destructive (McGehee *et al.*, 1998). Thus, at angles away from normal incidence, the phases of the backscattered signals from each element are very important to the summation in Equation (3). There is variability in the phases of scatter from scattering elements of the krill because:

1. scattering in a field with noise is a stochastic process;
2. krill have shapes that are more complex than juxtapose cylinders of varying radii; and
3. their bodies flex as they swim.

To account for these realities in the model, phase variability is added to each element j of f_{bs}, and a stochastic version of the DWBA is thus introduced (SDWBA). The form function accounting for phase variability in the scattered signal from each element is

$$f_{bs}(\theta) = \sum_{j=1}^{N} f_{bs_j}(\theta)\exp(i\varphi_j). \tag{4}$$

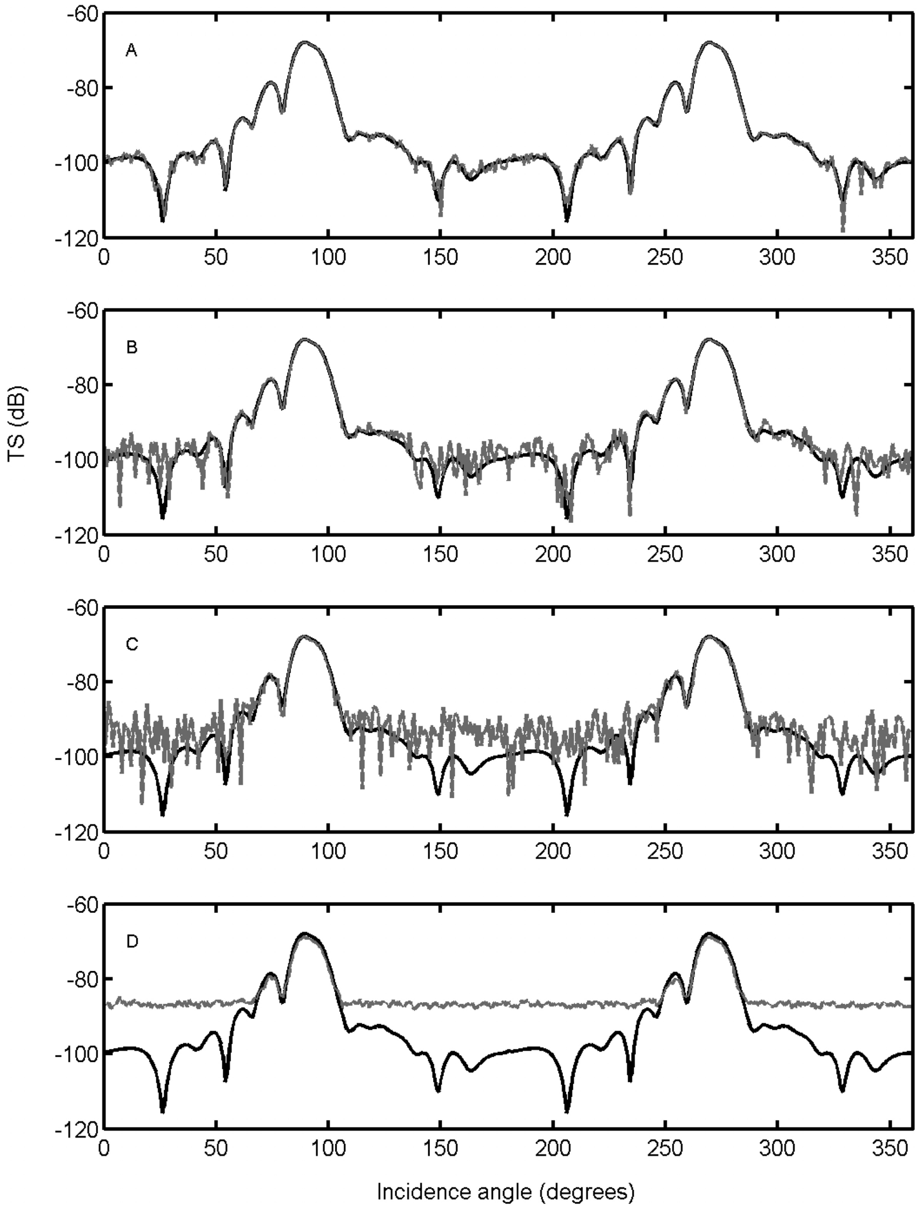

Figure 3. The DWBA model solved with the generic krill shape, g = 1.0357 and h = 1.0279 (black lines), and the stochastic DWBA model (SDWBA) solved with different values of phase-variability (gray lines; sd(φ) = 0.0224, 0.0707, 0.2236 and 0.7071 radians from A–D, respectively). The expected values of TS in the SDWBA are computed from σ_{bs} averaged over 100 realizations of the random phase.

As usual, the backscattering cross-sectional area and TS are

$$\sigma_{bs}(\theta) = |f_{bs}(\theta)|^2, \tag{5}$$

and

$$TS(\theta) = 10\log_{10}(\sigma_{bs}(\theta)), \tag{6}$$

respectively. As previously mentioned, the phase variance is attributed to noise, plus shape complexities, plus flexure. To quantify the minimum expected phase variability (e.g. that due to noise only), the variance of phase in Gaussian noise is described in Demer *et al.* (1999)

$$\mathrm{var}[\varphi_j] = \frac{1}{2\mathrm{SNR}} \tag{7}$$

where SNR is the signal-to-noise power ratio. Note that the actual phase variability will be greater than this due to the generally unknowable effects of complexities in body shape, internal structure, and flexure. Thus, the expected value for target strength (E[TS(θ)]) is estimated by averaging σ_{bs} over multiple realizations of phase variability at a fixed sd[φ_j] (Table 1). Because the krill TS data in McGehee *et al.* (1998) were measured using a 0.5 ms pulse duration (τ), E[TS(θ)] is also averaged with a 2 kHz bandpass filter (bandwidth ∼ 1/τ).

Results

Using Equations (4–7), the E[TS(θ)] is calculated for all θ (1° resolution) using 100 realizations of phase selected randomly from a Gaussian distribution. This is repeated for sd[φ_j] = 0.0224, 0.0707, 0.2236, and 0.7071 radians (rd) (Figure 3). For sd[φ_j] = 0.0224 rd, the phase-noise has negligible effect on the DWBA model at any incidence angle. However, as the sd[φ_j] is decreased to 0.0707 rd, the main lobe is unchanged while the side-lobes of TS(θ) begin to disappear. The addition of phase variability (sd[φ_j] = 0.2236 and then 0.7071 rd) causes the TS values at angles away from the main lobe to increase dramatically to relatively constant levels more than 10 dB above the noise floor in the experiments of McGehee *et al.* (1998). Again, the main lobe is virtually unaffected by phase variability.

Table 1. The standard deviation (sd) of phase versus SNR in decibels for Gaussian noise from Demer *et al.* (1999). As phase variability is the result of noise, complex and dynamic animal shapes, and general randomness in sound scatter, these sd are interpreted as minimum values at each SNR.

SNR (dB)	sd(φ) (radians)	sd(φ) (degrees)
30	0.0224	1.3
20	0.0707	4.1
10	0.2236	12.8
5	0.3976	22.8
0	0.7071	40.5

The krill TS from Animal 1 of McGehee *et al.* (1998) are overlaid on the SDWBA model computed with sd[φ_j] = 0.7071 rd (Figure 4). With or without taking into account phase variability, the matches between the TS measurements and DWBA model predictions remain unchanged on the main scattering lobe. However, in the

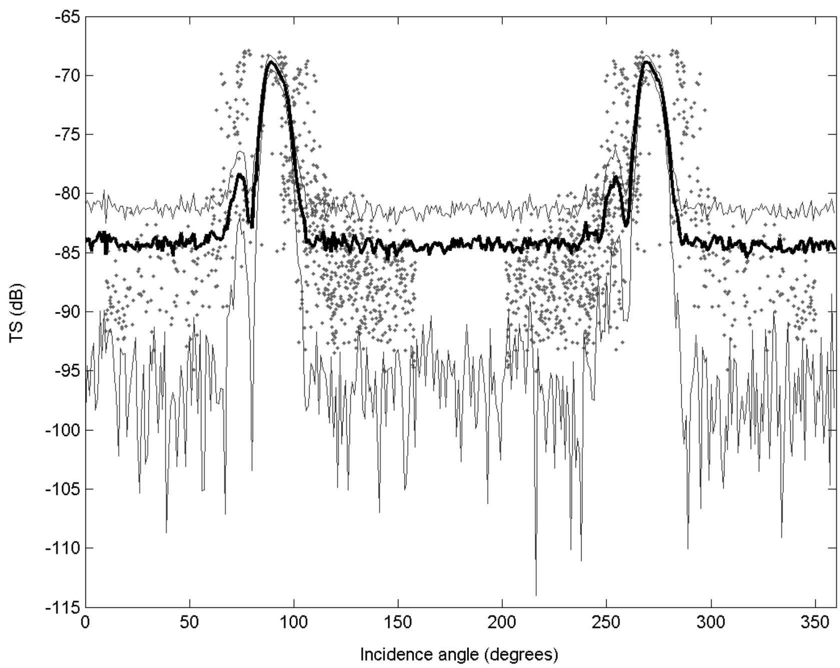

Figure 4. The SDWBA model (black line) computed with sd(φ) = 0.7071 rd and a 2 kHz bandwidth filter. The experimental data (dots) are almost completely bounded by the ±1sd error bounds of the SDWBA model (gray lines).

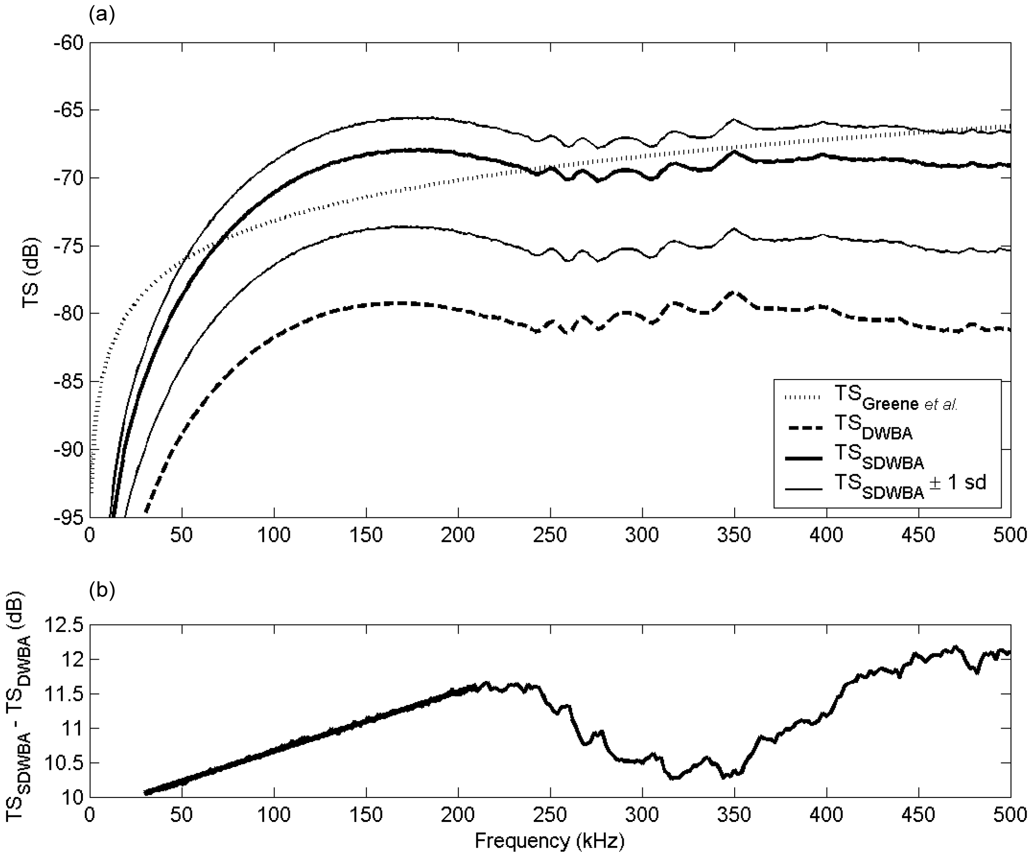

Figure 5. A comparison (a) of the Greene *et al.*, DWBA and SDWBA models for L = 31.6 mm. The first model is frequency transformed (Greene *et al.*, 1991), and the latter two models are averaged over $\theta = N(45.3°, 30.4°)$. Differences between the SDWBA and DWBA models are also shown (b). For rapid computation of $E[TS_{SDWBA}]$ below 210 kHz, the linear approximation for the differences between the probabilistic SDWBA model and the deterministic DWBA model is $\Delta TS = 0.0086f + 9.7924$ dB.

side-lobes the SDWBA model is a much better match to the empirical TS data than the DWBA model.

The significance of the new SDWBA model can be appreciated by overlaying the SDWBA ± 1sd, DWBA, and Greene *et al.* models (Figure 5). SDWBA predicts krill TS that are about 10–12 dB greater than those predicted by the SDWBA. Below 210 kHz, the differences between the two models increase linearly with frequency. Comparing the SDWBA model and Greene *et al.* model, the differences are either positive or negative, depending upon the frequency. As the Greene *et al.* model does not account for scattering in the Rayleigh regime (Wiebe *et al.*, 1990), the differences between these two models increase greatly at lower frequencies (below about 50 kHz).

Conclusions

Phase variability in the scatter from elements of a discretized-bent cylinder causes a dramatic flattening or plateau in the side-lobe regions of the DWBA model, while negligibly affecting the main scattering lobe. These results are consistent with the krill TS measurements in McGehee *et al.* (1998). Thus, by accounting for the stochastic nature of sound scattering in the solution of the DWBA model, the SDWBA model (Figure 5) provides a more accurate tool for predicting krill TS as a function of acoustic frequency, and animal size (generic shape; McGehee *et al.*, 1998), g (Foote *et al.*, 1990), h (Foote, 1990), and orientation (Kils, 1981). Although the SDWBA model is probabilistic and therefore predicts TS within a range of about 8 dB (E[TS(f)]±1sd), the expected values (E[TS(f)]) are approximately −5.7, 2.3, and 3.3 dB different from the deterministic Greene *et al.* model predictions at 38, 120, and 200 kHz, respectively (typical survey frequencies). Before the important ramifications of these conclusions are discussed, the SDWBA model should be validated using scattering data from many krill collected over a broad-bandwidth (see Demer and Conti, in press).

Acknowledgements

We are appreciative of the United States Antarctic Marine Living Resources Program, for funding this investigation.

Special thanks to Professor Duncan McGehee, Cuyamaca College, for providing the krill TS data for Animal 1 and information about the pulse duration used to record the measurements in McGehee *et al.* (1998).

References

Demer, D. A. An estimate of error for the CCAMLR 2000 estimate of krill biomass. CCAMLR. 2000. Special Issue Deep Sea Res (in press).

Demer, D. A., and Martin, L. V. 1995. Zooplankton target strength: volumetric or areal dependence? Journal of the Acoustical Society of America, 98(2 Pt. 1): 1111–1118.

Demer, D. A., and Conti, S. G. Broadbandwidth total target strength measurements of Antarctic krill *Euphausia superba* from reverberation in a cavity. ICES Journal of Marine Science (in press).

Demer, D. A., Soule, M. A., and Hewitt, R. P. 1999. A multiple-frequency method for potentially improving the accuracy and precision of *in situ* target strength measurements. Journal of the Acoustical Society of America, 105(4): 2359–2376.

Foote, K. G. 1990. Speed of sound in *Euphausia superba*. Journal of the Acoustical Society of America: 87(4): 1405–1408.

Foote, K. G., Everson, I., Watkins, J. L., and Bone, D. G. 1990. Target strengths of Antarctic krill (*Euphausia superba*) at 38 and 120 kHz. Journal of the Acoustical Society of America, 87(1): 16–24.

Greene, C. H., Stanton, T. K., Wiebe, P. H., and McClatchie, S. 1991. Acoustic estimates of Antarctic krill. Nature, 349: 110.

Hewitt, R. P., and Demer, D. A. 1991. Krill abundance. Nature, 353: 310.

Hewitt, R. P., Watkins, J. L., Naganobu, M., Tshernyshkov, P., Brierley, A. S., Demer, D. A., Kasatkina, S., Takao, Y., Goss, C., Malyshko, A., Brandon, M. A., Kawaguchi, S., Siegel, V., Trathan, P. N., Emery, J. H., Everson, I., and Miller, D. G. M. 2002. Setting a precautionary catch limit for Antarctic krill. Oceanography, 15(3): 26–33.

Kils, U. 1981. The swimming behavior, swimming performance and energy balance of Antarctic krill, *Euphausia superba*. BIOMASS Scientific Series No. 3, 122 pp.

McGehee, D. E., O'Driscoll, R. L., and Martin Traykovski, L. V. 1998. Effects of orientation on acoustic scattering from Antarctic krill at 120 kHz. Deep Sea Research Part II, 45: 1273–1294.

Morse, P. M., and Ingard, K. U. 1968. Theoretical Acoustics. Princeton University Press, Princeton, NJ. 927 pp.

SC-CAMLR. 1991. Report of the 10th Meeting of the Scientific Committee (SC-CAMLR-X), Hobart, Australia. 427 pp.

Stanton, T. K., Chu, D., and Wiebe, P. H. 1998. Sound scattering by several zooplankton groups. II: Scattering models. Journal of the Acoustical Society of America, 103: 236–253.

Wiebe, P. H., Greene, C. H., Stanton, T. K., and Burczynski, J. 1990. Sound scattering by live zooplankton and micronekton: empirical studies with a dual-beam acoustical system. Journal of the Acoustical Society of America, 88(5): 2346–2360.

ICES Journal of Marine Science, 61: 157–158. 2004
doi:10.1016/j.icesjms.2003.12.003

Erratum

ICES Journal of Marine Science, 60: 429–434. 2003[☆]

Reconciling theoretical versus empirical target strengths of krill: effects of phase variability on the distorted-wave Born approximation

David A. Demer and Stéphane G. Conti

In the caption for Figure 5, it was erroneously stated that the TS curves were normalized to $L = 31.6$ mm. They were normalized to $L = 38.35$ mm. Also, in the computations for Figure 5, the 100 realizations of TS_{SDWBA} were too large, by a factor of 4π, and were averaged in the logarithmic domain. In the revised computations and figure, the 100 realizations of TS_{SDWBA} have been averaged in the linear domain, and the 4π error was corrected. Cascading from these corrections, the $TS_{SDWBA} - TS_{DWBA}$ curve has been decreased by approximately 11 dB; the curve fit is $\Delta TS = 0.01414f - 1.02044$ dB; and the expected values ($E[TS_{SDWBA}(f)]$) are approximately -15.4, -7.5, and -7.9 dB different from the deterministic Greene *et al.* model predictions at 38, 120, and 200 kHz, respectively. The revised Figure 5 is printed overleaf.

In the Conclusions section on p. 433, the second-from-last line should read:
Although the SDWBA model is probabilistic and therefore predicts TS within a range of about 8 dB ($E[TS_{SDWBA}(f)] \pm$ 1 s.d.), the expected values ($E[TS_{SDWBA}(f)]$) are approximately -15.4, -7.5, and -7.9 dB different from the deterministic Greene *et al.* model predictions at 38, 120, and 200 kHz, respectively (typical survey frequencies).

[☆] doi of original article 10.1016/S1054-3139(03)00002-X

1054-3139/$30 Published by Elsevier Ltd on behalf of International Council for the Exploration of the Sea.

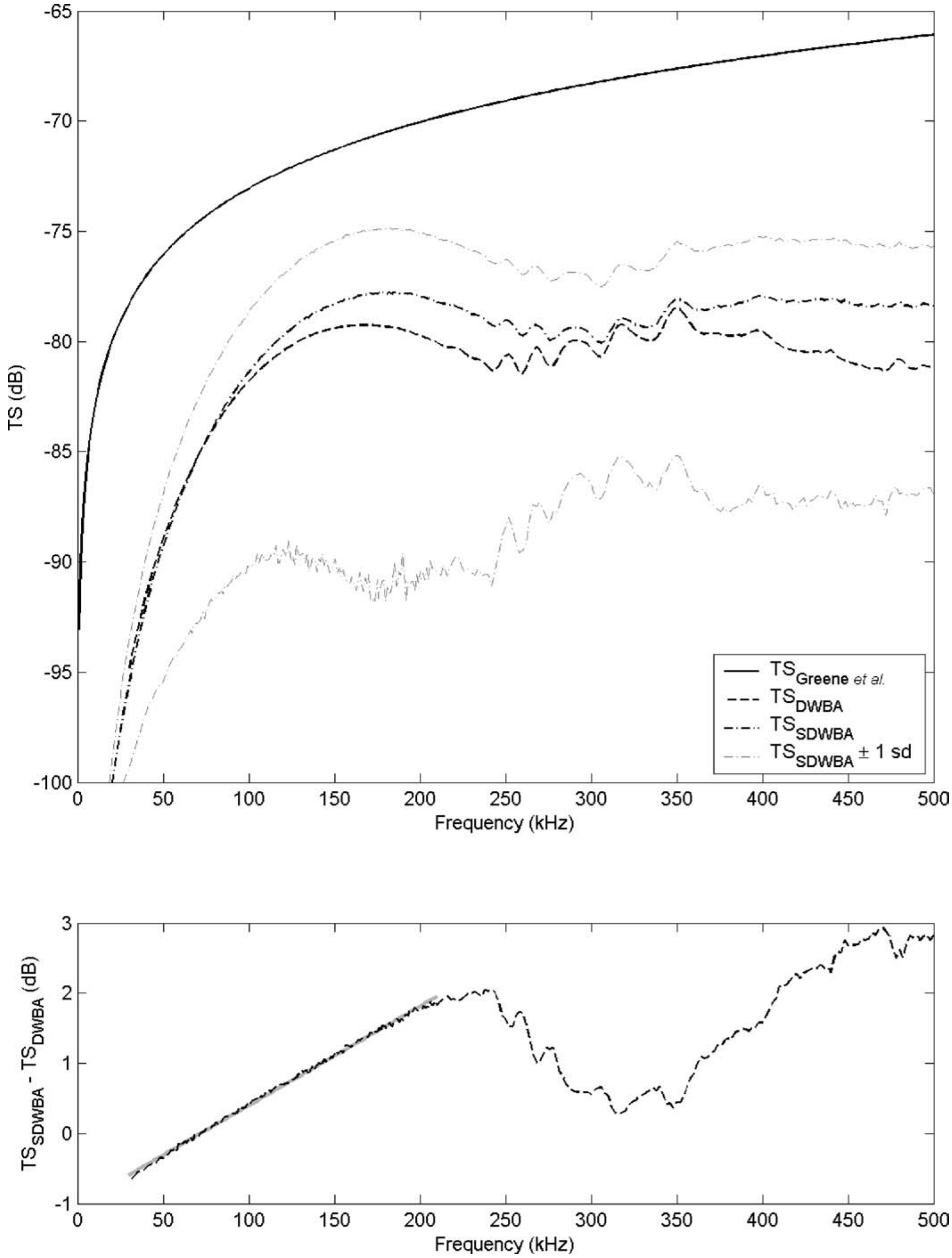

Figure 5. A comparison (a) of the Greene *et al.*, DWBA and SDWBA models for $L = 38.35$ mm. The first model is frequency transformed (Greene *et al.*, 1991), and the latter two models are averaged over $\theta = N(45.3°, 30.4°)$. (b) Differences between the SDWBA and DWBA models are also shown. For rapid computations of $E[TS_{SDWBA}(f)]$ below 210 kHz, the linear approximation for the differences between the probabilistic SDWBA model and the deterministic DWBA model is $\Delta TS = 0.01414f - 1.02044$ dB.